Geophysical Research Letters

RESEARCH LETTER
10.1029/2021GL096392

Can IMERG Data Capture the Scaling of Precipitation Extremes With Temperature at Different Time Scales?

Seyed-Mohammad Hosseini-Moghari[1] **and Qiuhong Tang**[1,2]

[1]Key Laboratory of Water Cycle and Related Land Surface Processes, Institute of Geographic Sciences and Natural Resources Research, Chinese Academy of Sciences, Beijing, China, [2]University of Chinese Academy of Sciences, Beijing, China

Key Points:

- Integrated Multi-satellite Retrievals for Global Precipitation Measurement (IMERG) represents well the relationship between precipitation extremes and temperature at 6-hourly and daily scales
- IMERG's scaling factors in dry areas are closer to the observations than in wet regions
- IMERG overestimates (underestimates) hourly precipitation extremes at low (high) temperatures

Supporting Information:

Supporting Information may be found in the online version of this article.

Correspondence to:

Q. Tang,
tangqh@igsnrr.ac.cn

Citation:

Hosseini-Moghari, S.-M., & Tang, Q. (2022). Can IMERG data capture the scaling of precipitation extremes with temperature at different time scales? *Geophysical Research Letters*, *49*, e2021GL096392. https://doi.org/10.1029/2021GL096392

Received 28 SEP 2021
Accepted 18 JAN 2022

Author Contributions:

Conceptualization: Seyed-Mohammad Hosseini-Moghari, Qiuhong Tang
Data curation: Seyed-Mohammad Hosseini-Moghari
Formal analysis: Seyed-Mohammad Hosseini-Moghari
Funding acquisition: Qiuhong Tang
Methodology: Seyed-Mohammad Hosseini-Moghari, Qiuhong Tang
Supervision: Qiuhong Tang
Writing – original draft: Seyed-Mohammad Hosseini-Moghari
Writing – review & editing: Qiuhong Tang

Abstract This study evaluates the validity of the Integrated Multisatellite Retrievals for Global Precipitation Measurement (IMERG) in scaling extreme precipitation with temperature (termed scaling factor, SF). To this end, we use Hadley-Integrated Surface Database (HadISD) data set at 1-hourly, 6-hourly, and 24-hourly scales between 2000 and 2020 over the contiguous United States (CONUS) as a reference data set. Our findings reveal that IMERG can capture changes in precipitation extremes with the temperature at 6-hourly, and 24-hourly scales, especially over dry regions. The difference between IMERG's SF and HadISD's SF at 6-hourly scale is less than 0.3%/°C in dry areas. However, IMERG underestimates SF in wet regions, especially at 1-hourly scale, up to ∼5%/°C. It is found that IMERG's performance is dependent on temperature, particularly at 1-hourly scale. IMERG overestimates extreme precipitations when temperatures are below 5°–11°C while the opposite is true at higher temperatures, indicating the need for considering temperature in adjusting IMERG.

Plain Language Summary Understanding the scaling rate of precipitation extremes with temperature can help to estimate precipitation extremes under global warming. However, we do not have in situ precipitation data in many parts of the world to monitor changes in precipitation extremes with temperature. The remotely sensed precipitation data sets that are available globally with high spatio-temporal resolution might be excellent resources to use for this purpose. To discover that, in this study, we evaluated the performance of the Integrated Multisatellite Retrievals for Global Precipitation Measurement (IMERG) as one of the newest precipitation data sets for scaling extreme precipitation with temperature over the contiguous United States. We compared IMERG's results with Hadley-Integrated Surface Database results at 1-hourly, 6-hourly, and 24-hourly scales. Results indicate IMERG has a considerable performance at 6-hourly and 24-hourly time scales.

1. Introduction

Given the thermodynamic Clausius-Clapeyron (CC) relationship, the moisture-holding capacity of the atmosphere increases by ∼7% per degree of warming (Fujibe, 2013; Trenberth et al., 2003). Assuming the constant relative humidity, the actual air humidity rises simultaneously (Ali et al., 2021), resulting in heavier precipitation at higher temperatures (Schroeer & Kirchengast, 2018). This increase in precipitation rate would increase the risk of flash floods and landslides, threatening socio-economic infrastructures (Fadhel et al., 2018; Fowler et al., 2021). Therefore, in order to planning and socio-economic decision-making, there is a clear need to understand how the extreme precipitation responds to an increase in temperature (Ali et al., 2021; Fowler et al., 2021).

Many regional and global studies attempted to estimate the rate of increase in precipitation intensity with rising temperature (e.g., Ali et al., 2018; Lenderink et al., 2021; Vergara-Temprado et al., 2021; W. Zhang et al., 2019). This rate, called scaling factor (SF), is affected by many factors such as precipitation duration and type, seasonality, large-scale circulations (Berg et al., 2009; Panthou et al., 2014; Pumo & Noto, 2021). However, studies generally agree on higher SF in shorter durations (Ali et al., 2021; Fowler et al., 2021; Lenderink & van Meijgaard, 2008).

Despite the large body of work on the extreme precipitation-temperature relationship, its understanding entirely remains an open question over many regions due to several reasons, including data availability issue that is, the low number of observation sites. Under this circumstance, finding a new source of information is vital. Remotely sensed precipitation data is one potential data source that could be applied in this find (Ali et al., 2021; Fowler et al., 2021). Nowadays, several institutions work on the precipitation estimation using remotely sensed data

resulting in various precipitation products with an acceptable spatio-temporal resolution, for example, Tropical Rainfall Measuring Mission (TRMM; Huffman et al., 2007) Climate Prediction Center morphing technique (CMORPH.; Joyce et al., 2004), Precipitation Estimation from Remotely Sensed Information Using Artificial Neural Networks (PERSIANN; Sorooshian et al., 2000). Although, these data show noteworthy potentials in several fields, for example, drought monitoring, extreme precipitation analysis, hydrological modeling, etc. (Caloiero et al., 2021; DaSilva et al., 2021; Jiang et al., 2021; Le et al., 2020; Liu et al., 2020; Zubieta et al., 2017), their performance in analyzing the relationship between precipitation extremes and temperature is unknown.

One of the latest satellite-based precipitation products is the Integrated Multisatellite Retrievals for Global Precipitation Measurement (IMERG, G. J. Huffman et al., 2015). This data set has attracted attention to be applied in the majority of fields due to its unique features, that is, high spatial ($0.1° \times 0.1°$) and temporal (30 min) resolution, full coverage of the globe, available to the public free of charge and without any restrictions, providing around 20-year data almost without any gap, and relatively short latency (Hosseini-Moghari & Tang, 2020). These features make the IMERG an attractive alternative for in situ data in assessing the extreme precipitation-temperature relationship. However, before jumping to any conclusions based on the IMERG information, we should keep in mind that there is no guarantee for the validity of its data. And understanding its error characteristics and its validity is vital before using that in operational applications. Therefore, this question remains open that how IMERG performs in scaling extreme precipitation with temperature at subdaily scale. To fill this gap, in this study, we focus on quantifying IMERG's capability to scale precipitation extreme at 1-hourly and 6-hourly time scales as well as at the daily scale. To this end, we use HadISD (Hadley-Integrated Surface Database) data set as a reference for evaluating IMERG performance in different spatio-temporal scales over the contiguous United States (CONUS). The rest of this paper is structured into three sections. In Section 2, the employed data and the Methods of the study are presented in detail. The results and discussion are shown in Section 3. At the end, conclusions are presented in Section 4.

2. Data and Methods

2.1. HadISD Data Set

HadISD is a station-based data set of meteorological variables based on data from the ISD (Smith et al., 2011) handed out by the Met Office Hadley Centre (Dunn et al., 2012). This data set offers observed subdaily data for significant parts of the world to study past extremes events (Dunn et al., 2016). HadISD Includes more than 8,000 stations worldwide, mainly over North America and Europe (Molina et al., 2021). This data set embraces several meteorological variables (see Table 4 in Dunn et al., 2016). Here, we obtained precipitation and dew point temperature (DPT) data from its current version (version 3.1.1.2020f). Although this data set covers 1931–2020 (for a small proportion of stations), we used HadISD data from June 2000 to November 2020 to be consistent with IMERG data. We considered only those stations with at least 10 years of data and no less than 1,212 events.

It should be noted that due to the goal of this study, time continuity is not a concern. After applying these filters, only the number of stations with 1-hr, 6-hr, and 24-hr reports was considerable over North America and some parts of Europe. Therefore, we consider the CONUS as a case study in this paper. Later, we checked the quality of the data in terms of outliers, negative value, and consistency in reporting different subdaily scales, for example, 6-hr precipitation events equal or greater than 1-hr events in the same period. Ultimately, from more than 1,200 stations over the US, we have 848 stations at 1-hourly scale, 762 stations at 6-hourly scale, and 627 stations at 24-hourly scale. We did not calculate 24-hr data from 1-hr or 6-hr data because of existing gaps. Therefore, the number of stations with 1-hr and 6-hr reports is more than 24-hr due to having more events.

2.2. IMERG Data Set

IMERG is a unified algorithm developed by Huffman et al. (2015) to estimate the precipitation based on observations from Global Precipitation Measurement (GPM) and a multinational constellation of satellite-borne microwave radiometers. IMERG freely offers 30-min precipitation with a spatial resolution of $0.1° \times 0.1°$ (Skofronick-Jackson et al., 2017). Until the fifth version, IMERG includes only the GPM era. Later, in version 6, the IMERG was applied on TRMM observations to extend back the starting date from March 2014 to June 2000 (Hosseini-Moghari & Tang, 2020). IMERG includes three types of products, that is, early, late, and final runs with a time latency of 4-hr, 12-hr, and 3.5 months, respectively (Tan et al., 2019). Currently, the final run

is adjusted using the Global Precipitation Climatology Centre (GPCC) data set at a monthly scale (Huffman et al., 2015). There is a possibility of shared stations between GPCC and HadISD data sets resulting in IMERG and HadISD data sets may not be fully independent. However, due to the fact that the IMERG adjustment is made at a monthly scale and our analysis is done at daily and sub-daily scales, as well as the much higher spatial resolution of IMERG than GPCC, we assumed that the possible overlap of the two data sets would not affect the comparison results. In this study, we obtained 30-min precipitation data from IMERG version 6 final run over the CONUS from June 2000 to November 2020. Then, we extracted the IMERG data at each station's location and generated 1-hr, 6-hr, and 24-hr precipitation data from 30-min data for the same periods that each station has data.

2.3. Methods

The binning approach was used to estimate precipitation sensitivity with temperature (Lenderink & van Meijgaard, 2008; X. Zhang et al., 2017). We considered the pairs of DPT and precipitation in wet hours (with precipitation ≥0.1 mm) to analyze the precipitation-temperature relationship. We sorted the pairs DPT and precipitation in ascending order by DPT and then put them into 12 bins with an equal number of pairs (Herath et al., 2018). Also, the stations with less than 1,212 events were excluded from the calculations, that is, no less than 100 events per bin were considered. Mean DPT and the 99th percentile of precipitation ($P99^{th}$) were calculated for each bin. The first and last bins were excluded from the SF calculation to deal with the specific atmospheric circulation influence on very low and very high DPT values (Ali et al., 2021). Then, a linear regression (Equation 1) was fitted to the $P99^{th}$ and mean DPT vector for each station (Ali & Mishra, 2017; Ali et al., 2018; Bui et al., 2019):

$$\ln(P99^{th}) = \alpha\overline{DPT} + \beta \quad (1)$$

$$SF = 100 \times [\exp(\alpha) - 1], \quad (2)$$

where $\overline{DPT}$ is mean DPT (°C), α and β denote slope and intercept of the linear regression, respectively; and SF is scaling of precipitation with temperature (%/°C). It should be noted that to cap the significant impact of the cooling effect on SF in the tropical area, SFs were calculated based on antecedent DPT (DPT before a precipitation event) for those stations located in this climate (Hosseini-Moghari et al., 2022; Visser et al., 2020).

We divided the stations into two categories, that is, stations lie in wet and dry regions based on the wet/dry classification map from Donat et al. (2016). Donat et al. (2016) provided two precipitation-based wet/dry classification maps based on the total annual precipitation (PRCTOT) and the annual-maximum daily precipitation (Rx1day) indices. In their map, one cell is considered as a wet (dry) cell if its normalized index (i.e., PRCTOT or Rx1day) is among the 30% highest (lowest) normalized index values. More information about wet and dry regions can be found in Donat et al. (2016). Moreover, due to the notable impact of climate on precipitation's scaling with temperature (Panthou et al., 2014), we split the CONUS into four main climatic regions, that is, arid, cold, temperate, and tropical climate zones based on the Köppen-Geiger climate classification map from Beck et al. (2018) (see Figure S1 in Supporting Information S1). It needs to be noted that climate is an imprecise proxy for precipitation types and morphologies that occur in a regime. Indeed, some types of precipitating systems directly and continuously scale with increasing humidity and temperature, and some do not. Mesoscale convective systems, for example, do not simply or continuously scale with convective available potential energy because they are also strongly related to the environmental wind shear and terrain (if any) forcing. Hence, it can be a potential source for uncertainty and reduce the accuracy of our results. However, it can be assumed that its impact on the results of both data sets is almost similar; therefore, the comparison would be valid. The number of stations in arid, cold, temperate, and tropical climates is 177 (148/107), 337 (312/274), 328 (292/242), and 6 (10/4) stations for 1-hr (6-hr/24-hr) time scale, respectively. We also calculated SFs by randomly removing 25% and 50% of stations in each climate zone (except tropical) to see how SF is sensitive to the number of stations. Results did not show a considerable difference indicating the robustness of sample size (see Figure S2 in Supporting Information S1).

To generate the extreme precipitation-temperature curves, inspired by Lenderink et al. (2021), we grouped all stations with elevation above and below 400 m in each climate zone. This separation helps avoiding artificially flat curves by dealing with the DPT mixing from different elevations (Ali et al., 2021). Then, we put all data pairs of precipitation and positive DPT of all stations in a climate zone and an elevation class together to generate a precipitation-temperature curve based on 12 bins with an equal number of pairs. Due to the low number of stations in tropical areas, the curves were not plotted for this climate. Finally, in addition to $P99^{th}$, we analyzed

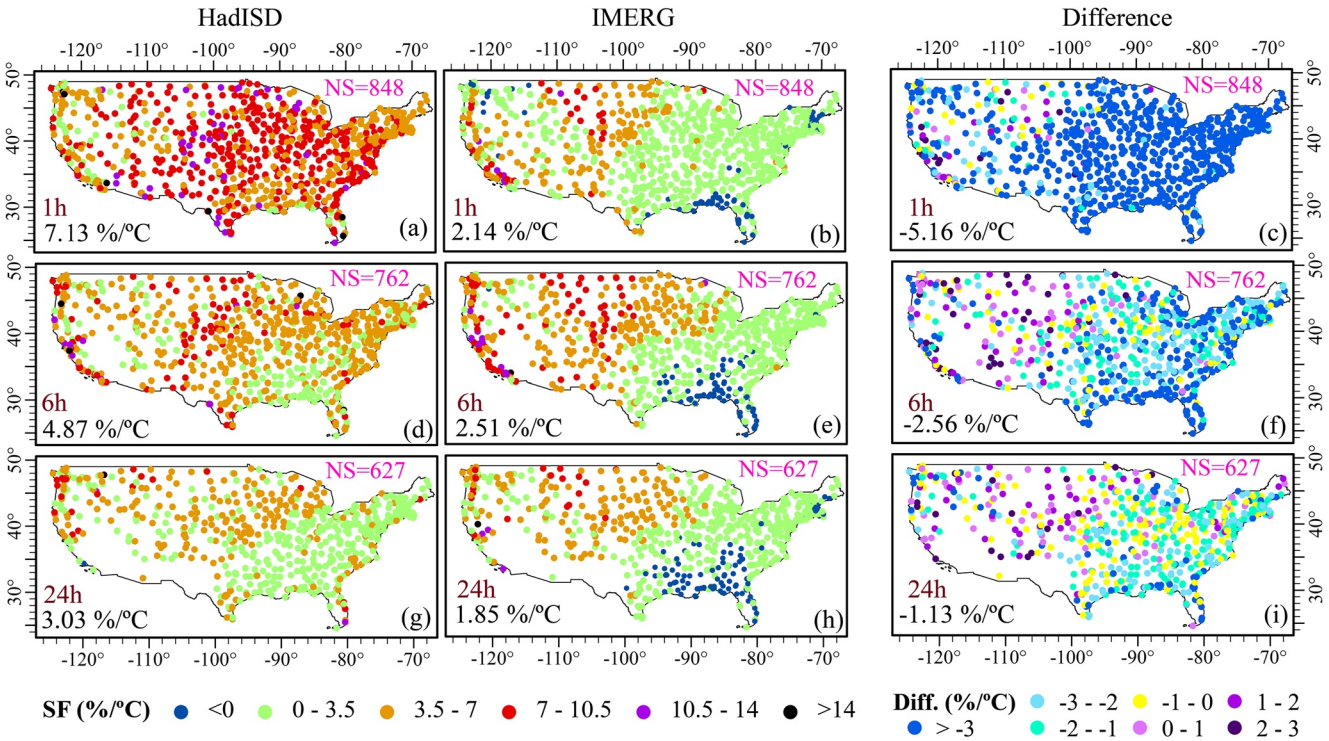

Figure 1. Scaling factors (SFs) for the 99th percentile of (a and b) 1-hourly, (d and e) 6-hourly, (g and h) and 24-hourly precipitation from the Hadley-Integrated Surface Database (HadISD; left column) and Integrated Multi-satellite Retrievals for Global Precipitation Measurement (IMERG; middle column) datasets using dew point temperature. The right column indicates the difference between IMERG's SFs and HadISD's SFs at (c) 1-hourly, (f) 6-hourly, and (i) 24-hourly time scale. The pink and black numbers indicate the number of stations/pixels and median of SFs at each time scale, respectively.

changes in the rate of SF for the 50th, 75th, and 95th percentiles of precipitation data from HadISD and IMERG in different climate zones.

3. Results and Discussion

The spatial distribution of obtained SFs from HadISD and IMERG, as well as the difference between them over the CONUS was shown in Figure 1. First, we compared HadISD's results with the findings of Ali et al. (2021), who used the GSDR with more than 3,000 stations for scaling precipitation extremes over the CONUS. Ali et al. (2021) reported a median SFs of 6.2% and 3.3%/°C for 1-hourly and 24-hourly time scales. Here, we found a median scaling rate of 7.1% and 3.0%/°C at 1-hourly and 24-hourly time scales. The results of HadISD are similar to GSDR, and small differences can be related to the different number of stations used. Therefore, HadISD can be considered as truth for the IMERG assessment.

From Figure 1, in line with Vergara-Temprado et al. (2021), the median of obtained SFs from HadISD at 1-hourly scale (7.1%/°C) is close to our expectation from the CC relationship, that is, ~7%/°C. However, IMERG significantly underestimates SFs over the CONUS at 1-hourly scale, particularly in the east of the CONUS. The median of IMERG's SFs at 1-hourly scale is 2.1%/°C, well below CC-like scaling. The difference between the median of obtained SFs from IMERG at 1-hourly, and 24-hourly scales is 0.3%/°C. In comparison, this value is 4.1%/°C for HadISD, indicating that the variation of SFs of IMERG across time scales is significantly less than HadISD. Indeed, a decrease in SF rates is expected with increasing time scale (as reported in previous studies, e.g., Ali et al., 2021, Fowler et al., 2021, and Guerreiro et al., 2018). However, this decrease from 1-hourly to 24-hourly scale is not considerable in IMERG's results due to its poor performance in representing the scaling rate of 1-hourly scale. At the 6-hourly scale, SFs from IMERG have an almost similar pattern to HadISD in the center and the west of the CONUS, suggesting improvement in IMERG performance compared with the 1-hourly scale. This improvement continues with increasing time scale, that is, a similar SFs pattern almost over the whole CONUS (expect the south-east) at 24-hourly scale. The median difference between SFs obtained from IMERG

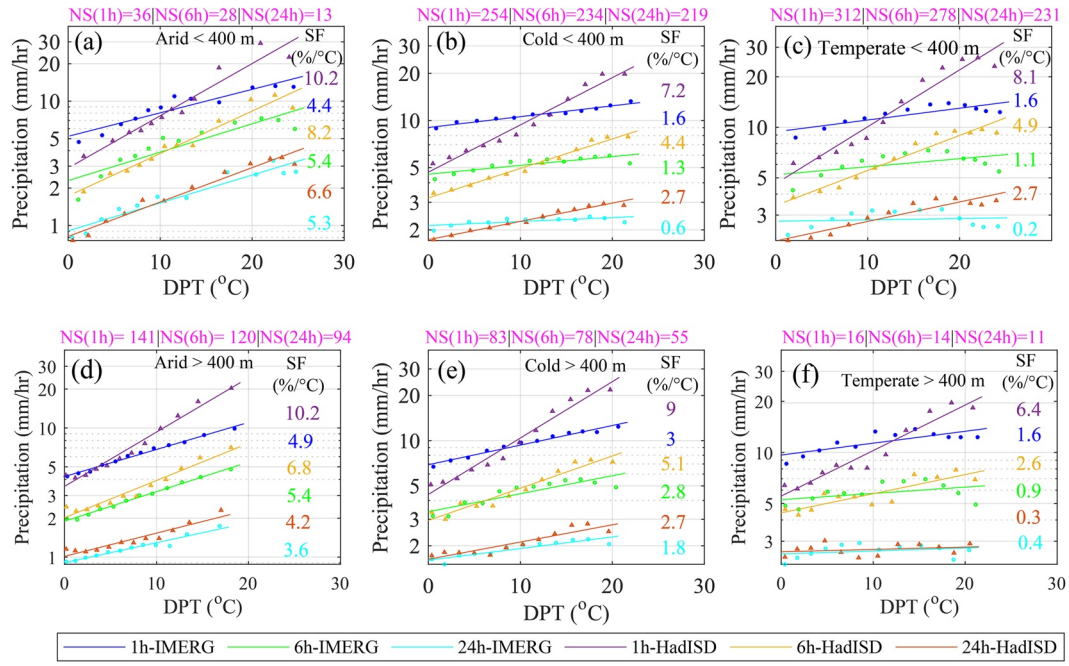

Figure 2. Relationship between the 99th percentile of precipitation at 1-hourly, 6-hourly, and 24-hourly time scale and dew point temperature based on the gauges/pixels at less and above than 400 m elevation in (a and d) arid, (c and e) cold, and (c and f) temperate climates. The pink numbers indicate the number of stations/pixels in each time scale. The inner color numbers show corresponding scaling factor to each line. The *y*-axis has a logarithmic scale. Note the tropical climate was excluded due to the limited number of stations.

and HadISD is only −1.1%/°C at 24-hourly scale. The reason for the poorer performance of IMREG at 1-hourly scale can be traced in the way of IMERG adjustment. IMERG final run is adjusted using monthly GPCC data (Huffman et al., 2015). Therefore, it is more likely that daily data get close to the observation values. However, an equal percentage of bias correction may be less helpful for hourly time scales, where the distribution of precipitation plays a vital role.

Unlike SFs that show the overall change of precipitation extremes with increasing the temperature as a single value, the precipitation extreme-temperature curves illustrate the change of precipitation extremes within the temperature range. Recall that the curves were not plotted for tropical regions due to the limited number of stations (see Section 2.3). According to Figure 2, scaling curves obtained from IMERG and HadISD are close at the daily scale, while their slopes are different at 1-hourly scale. Generally, precipitation extremes from IMERG are larger than HadISD for temperatures below 10°C, while the opposite is true for precipitation extremes at higher temperatures. Interestingly, Ali et al. (2021) reported the relatively low intensities for precipitation extremes (below CC-like scaling) over the Europe when DPT is below 10°C. Regardless of the precipitation intensities, the slope of precipitation extreme-temperature curves from IMERG in most cases (almost in all climates and all time scales) are close to HadISD, when DPT is below 10°C. It means that IMERG performs quite well, even at 1-hourly scale, within the DPT range below 10°C. Therefore, the poor performance of IMERG shown in Figures 1 and 2 at 1-hourly scale is mainly related to precipitation intensity in above 10°C, not the full range of DPT. This underestimation at higher temperatures can be partially explained by the fact that the number of short convective thunderstorms would increase at higher temperatures (Westra et al., 2014); under this circumstance, some events are likely not captured by satellites because of their limited numbers of overpasses (Tian et al., 2009).

We also examine SFs for other precipitation percentiles, that is, 50th, 75th, and 95th percentiles that all of them can not necessarily be considered as extreme events. However, this assessment can show the IMERG performance in estimating other important precipitation percentiles. Figure S3 in Supporting Information S1 shows the difference between the median of IMERG's SFs and HadISD's SFs in different climate zones and for different precipitation percentiles. Generally, SFs from IMERG are close (at 1-hourly scale) to HadISD or larger (at 6-hourly and 24-hourly time scales) than HadISD for 50th, 75th percentiles, while the opposite is true for 95th

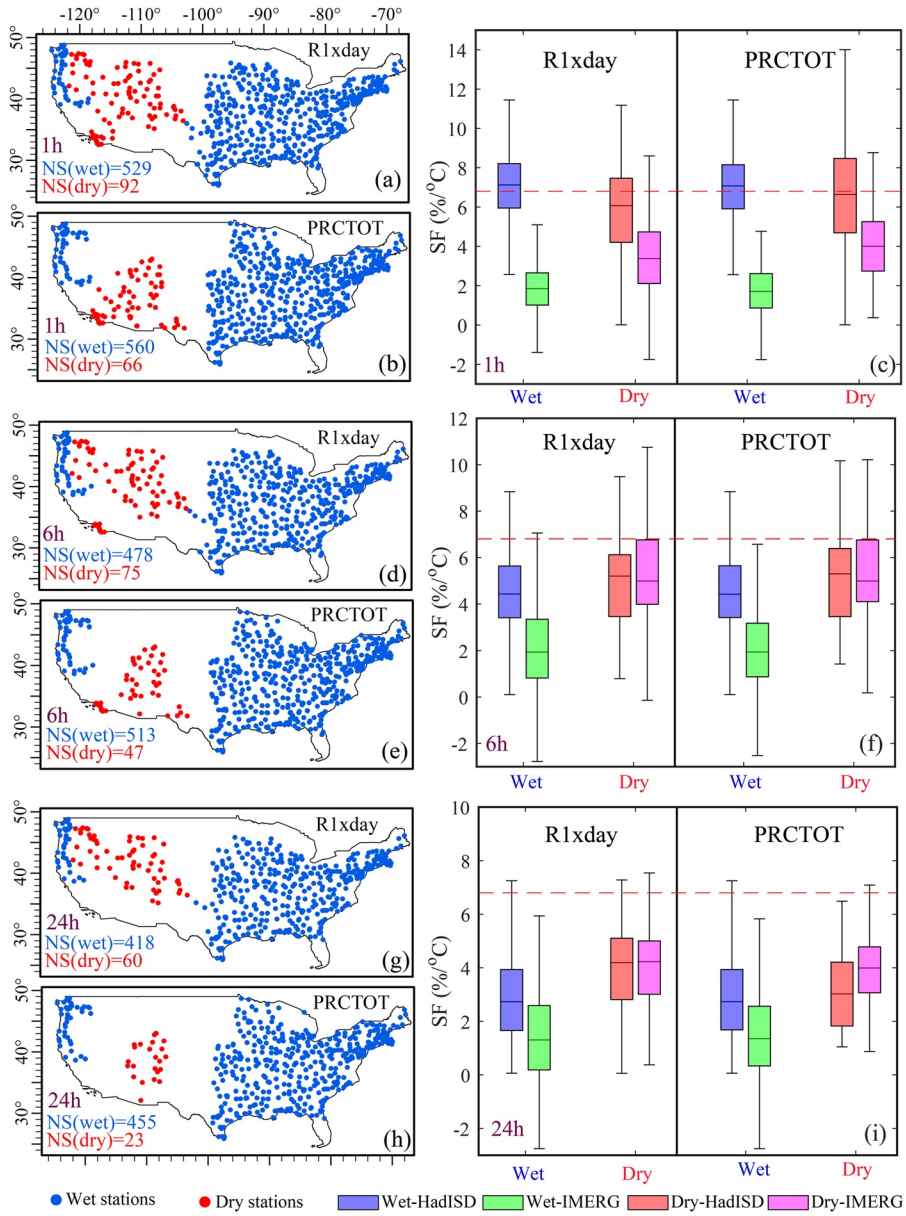

Figure 3. Distributions of stations in wet (blue) and dry (red) regions based on R1xday and PRCTOT indices along with boxplot of scaling factors obtained from Hadley-Integrated Surface Database and Integrated Multi-satellite Retrievals for Global Precipitation Measurement data sets in each region for (a, b, and c) 1-hourly, (d, e, and f) 6-hourly, (g, h, and i) 24-hourly precipitation events. The dashed red line indicates Clausius-Clapeyron like scaling of 6.8%/°C. The blue and red numbers indicate the number of stations/pixels in wet and dry regions at each time scale, respectively.

and 99th percentiles. IMERG performs better in arid areas, followed by cold regions almost in all time scales and all percentiles. The absolute differences between the median of IMERG's SFs and HadISD's SFs at all time scales are roughly less than 1%/°C for 50th and 75th percentiles; however, the differences can reach more than 5%/°C for 99th percentile at 1-hourly scale.

Figure 3 illustrates SFs from HadISD and IMERG in wet (blue) and dry (red) regions based on Donat et al. (2016)'s maps (see Section 2.3). From the figure, IMERG shows significantly a better performance in the dry areas, especially according to R1xday. Although the differences in the 1-hourly scale are still considerable, IMERG at 6-hourly and 24-hourly scales in dry regions perform quite similar to HadISD (see Figures 3c, 3f, and 3i). For example, the median of SFs in dry areas based on R1xday (PRCTOT) at 6-hourly scale is 5.2 (5.3) and 5.0

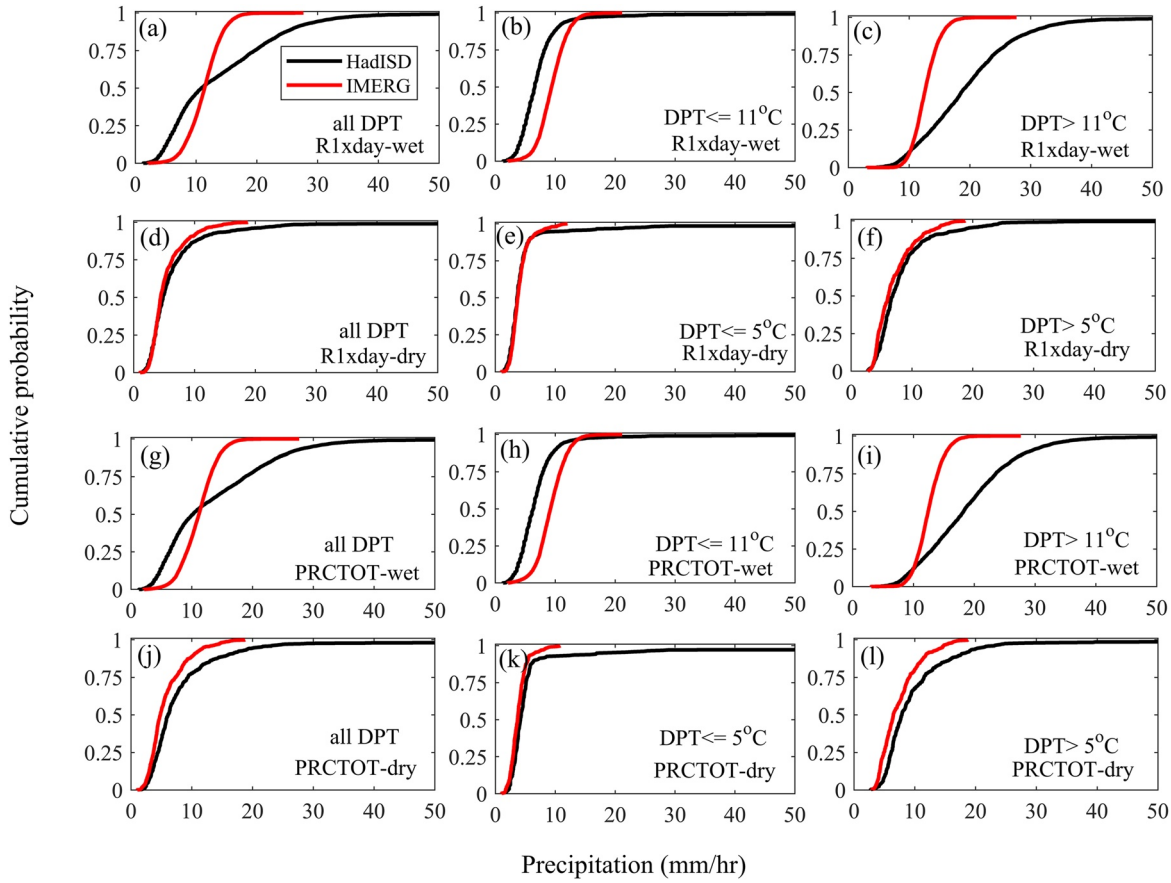

Figure 4. Empirical cumulative distribution function of the 99th percentile of 1-hourly precipitation for entire dew point temperatures range and temperature ranges below 11°C/5°C and above 11°C/5°C in wet/dry regions based on (a, b, and c) /(d, e, and f) R1xday and (g, h, and i)/(j, k, and l) PRCTOT, respectively.

(5.0) %/°C based on HadISD and IMERG, respectively. At 1-hourly scale, IMERG underestimates SFs and the underestimation in wet areas is higher than that in dry regions. Although underestimation remains in wet areas at 6-hourly and 24-hourly scales, IMERG does not underestimate SFs in the dry areas, and in some stations, it overestimates SF rates. It is likely that the poorer results in wet regions are related to the greater variety of precipitation types and morphologies in wet regions, including types less likely to scale directly and continuously with temperature and humidity (see Section 2.3). Based on both indices (i.e., R1xday and PRCTOT), the SFs from HadISD are higher for wet regions than dry areas at 1-hourly scale, while the opposite is true for 6-hourly and 24-hourly scales. Ali et al. (2021) reported a higher scaling rate at 1-hourly scale for dry areas based on R1xday globally, mainly due to a generally higher scaling rate over Europe.

Figure S4 in Supporting Information S1 shows the precipitation extreme-temperature curves in wet and dry regions. Similar to Figure 2, IMERG shows a different behavior at low and high temperatures in both regions. In wet (dry) areas, an overestimation of extreme precipitation is evident in IMERG data when the temperature is below 11–12°C (5–6°C), while the opposite is true for higher temperatures. Figure 4 illustrates the three empirical cumulative distribution functions (eCDF) for IMERG and HadISD extreme precipitation in each region corresponding to the entire temperature range, low temperatures, and high temperatures for 1-hourly time scale and Figures S5–S6 in Supporting Information S1 are for 6-hourly and 24-hourly time scales, respectively. The systematically overestimating and underestimating extreme precipitation at low and high temperatures is clear in the eCDFs, and the rate of underestimation is larger than overestimation, particularly in wet regions. It indicates that we would not be able to adjust IMERG with a conventional bias adjustment. The temperature should be considered in adjusting IMERG data with a higher adjustment ratio for higher temperatures. The development of such an adjustment approach is behind the scope of this study.

4. Conclusions

In this study, we used HadISD datasets to evaluate IMERG performance in scaling precipitation extreme with the temperature at 1-hourly, 6-hourly, and 24-hourly scales time scale over the CONUS. Based on our findings:

- IMERG can be an alternative for observed precipitation at 6-hourly and 24-hourly time scales, particularly over the west of the CONUS. However, in most cases, using IMERG data for scaling precipitation extremes at 1-shourly scale, especially over the east of the CONUS, leads to underestimation of scaling rate. Therefore, applying IMERG at 1-hourly scale should be done with caution. Moreover, IMERG performance increases with increasing the time scale.
- IMERG's performance is considerably better in the dry areas. IMERG performs pretty similarly to HadISD at 6-hourly and 24-hourly scales in dry regions. For example, at a 6-hourly time scale, the difference between the median of SFs from IMERG and HadISD is less than 0.3%/°C for stations that lie in dry areas. However, underestimation of SFs over wet areas exists at all time scales.
- There is a transition in IMERG's precipitation extremes estimations around 10°C over significant part of the CONUS (vary between 5° and 11°C in dry and wet regions). The IMERG estimates precipitation more than HadISD in DPT below 10°C and vice-versa for DPT above 10°C. The slopes of precipitation extreme-temperature curves from IMERG and HadISD are almost similar within DPT below 10°C and diverge at higher temperatures indicating that the poor performance of IMERG at 1-hourly scale is not related to the full range of temperature. It indicates the dependency of IMERG performance to the temperature suggesting that different adjustment ratios should be considered for adjusting IMERG data in low and high temperatures.
- Generally, the best performance of IMERG is seen in arid areas followed by cold regions. Moreover, IMERG, roughly with a maximum 1%/°C difference with HadISD, performs better in lower percentiles, that is, 50th and 75th percentiles, than higher percentiles. The rate of SFs based on IMERG is larger than the HadISD ones in the lower percentiles, while the opposite is true for upper percentiles.

The results of this study highlight the great potential of IMERG precipitation product as an alternative to in situ data for scaling precipitation extremes at 6-hourly and daily time scales. However, further improvement is recommended in adjusting IMERG data at 1-hourly scale. If the available sub-daily datasets like HadISD were used to adjust IMERG, it could enhance the applicability of this valuable data set at an hourly scale. Finally, it is worth mentioning that there are several other remotely sensed precipitation products available at sub-daily scale, such as the PERSIANN family, CMORPH, and GSMaP (Global Satellite Mapping of Precipitation; Kubota et al., 2007). Comparison and combination of these products may lead to a comprehensive understanding which is left to future studies.

Data Availability Statement

The HadISD data set is available at the Met Office Hadley Centre observations datasets (https://www.metoffice.gov.uk/hadobs/hadisd/, last accessed: 30 August 2021). The IMERG product is available through the NASA earth data portal (https://disc.gsfc.nasa.gov/, last accessed: 30 August 2021).

Conflict of Interest

The authors declare no conflicts of interest relevant to this study.

Acknowledgments
This study was funded by the National Natural Science Foundation of China (41790424, 41730645), the Strategic Priority Research Program of Chinese Academy of Sciences (XDA20060402), and the Chinese Academy of Sciences President's International Fellowship Initiative (2019VEA0019).

References

Ali, H., Fowler, H. J., Lenderink, G., Lewis, E., & Pritchard, D. (2021). Consistent large-scale response of hourly extreme precipitation to temperature variation over land. *Geophysical Research Letters*, *48*(4), e2020GL090317. https://doi.org/10.1029/2020GL090317

Ali, H., Fowler, H. J., & Mishra, V. (2018). Global observational evidence of strong linkage between dew point temperature and precipitation extremes. *Geophysical Research Letters*, *45*(22), 12320–12330. https://doi.org/10.1029/2018GL080557

Ali, H., & Mishra, V. (2017). Contrasting response of rainfall extremes to increase in surface air and dewpoint temperatures at urban locations in India. *Scientific Reports*, *7*(1), 1228. https://doi.org/10.1038/s41598-017-01306-1

Beck, H. E., Zimmermann, N. E., McVicar, T. R., Vergopolan, N., Berg, A., & Wood, E. F. (2018). Present and future Köppen-Geiger climate classification maps at 1-km resolution. *Scientific Data*, *5*(1), 180214. https://doi.org/10.1038/sdata.2018.214

Berg, P., Haerter, J. O., Thejll, P., Piani, C., Hagemann, S., & Christensen, J. H. (2009). Seasonal characteristics of the relationship between daily precipitation intensity and surface temperature. *Journal of Geophysical Research*, *114*, D18102. https://doi.org/10.1029/2009JD012008

Bui, A., Johnson, F., & Wasko, C. (2019). The relationship of atmospheric air temperature and dew point temperature to extreme rainfall. *Environmental Research Letters*, *14*(7), 074025. https://doi.org/10.1088/1748-9326/ab2a26

Caloiero, T., Caroletti, G. N., & Coscarelli, R. (2021). IMERG-based meteorological drought analysis over Italy. *Climate*, *9*(4), 65. https://doi.org/10.3390/cli9040065

DaSilva, N. A., Webber, B. G. M., Matthews, A. J., Feist, M. M., Stein, T. H. M., Holloway, C. E., & Abdullah, M. F. A. B. (2021). Validation of GPM IMERG extreme precipitation in the Maritime Continent by station and radar data. *Earth and Space Science*, *8*, e2021EA001738. https://doi.org/10.1029/2021ea001738

Donat, M. G., Lowry, A. L., Alexander, L. V., O'Gorman, P. A., & Maher, N. (2016). More extreme precipitation in the world's dry and wet regions. *Nature Climate Change*, *6*(5), 508–513. https://doi.org/10.1038/nclimate2941

Dunn, R. J. H., Willett, K. M., Parker, D. E., & Mitchell, L. (2016). Expanding HadISD: Quality-controlled, sub-daily station data from 1931. *Geoscientific Instrumentation, Methods and Data Systems*, *5*(2), 473–491. https://doi.org/10.5194/gi-5-473-2016

Dunn, R. J. H., Willett, K. M., Thorne, P. W., Woolley, E. V., Durre, I., Dai, A., et al. (2012). HadISD: A quality-controlled global synoptic report database for selected variables at long-term stations from 1973–2011. *Climate of the Past*, *8*(5), 1649–1679. https://doi.org/10.5194/cp-8-1649-2012

Fadhel, S., Rico-Ramirez, M. A., & Han, D. (2018). Sensitivity of peak flow to the change of rainfall temporal pattern due to warmer climate. *Journal of Hydrology*, *560*, 546–559. https://doi.org/10.1016/j.jhydrol.2018.03.041

Fowler, H. J., Wasko, C., & Prein, A. F. (2021). Intensification of short-duration rainfall extremes and implications for flood risk: Current state of the art and future directions. *Philosophical Transactions of the Royal Society A: Mathematical, Physical & Engineering Sciences*, *379*(2195), 20190541. https://doi.org/10.1098/rsta.2019.0541

Fujibe, F. (2013). Clausius-Clapeyron-like relationship in multidecadal changes of extreme short-term precipitation and temperature in Japan. *Atmospheric Science Letters*, *14*(3), 127–132. https://doi.org/10.1002/asl2.428

Guerreiro, S. B., Fowler, H. J., Barbero, R., Westra, S., Lenderink, G., Blenkinsop, S., et al. (2018). Detection of continental-scale intensification of hourly rainfall extremes. *Nature Climate Change*, *8*(9), 803–807. https://doi.org/10.1038/s41558-018-0245-3

Herath, S. M., Sarukkalige, R., & Nguyen, V. T. V. (2018). Evaluation of empirical relationships between extreme rainfall and daily maximum temperature in Australia. *Journal of Hydrology*, *556*, 1171–1181. https://doi.org/10.1016/j.jhydrol.2017.01.060

Hosseini-Moghari, S.-M., Sun, S., Tang, Q., & Groisman, P. Y. (2022). Scaling of precipitation extremes with temperature in China's mainland: Evaluation of satellite precipitation data. *Journal of Hydrology*, *606*, 127391. https://doi.org/10.1016/j.jhydrol.2021.127391

Hosseini-Moghari, S.-M., & Tang, Q. (2020). Validation of GPM IMERG V05 and V06 precipitation products over Iran. *Journal of Hydrometeorology*, *21*(5), 1011–1037. https://doi.org/10.1175/JHM-D-19-0269.1

Huffman, G. J., Bolvin, D. T., & Nelkin, E. J. (2015). Integrated Multi-satellitE Retrievals for GPM (IMERG) technical documentation. *NASA/GSFC Code*, *612*, 47.

Huffman, G. J., Bolvin, D. T., Nelkin, E. J., Wolff, D. B., Adler, R. F., Gu, G., et al. (2007). The TRMM Multisatellite Precipitation Analysis (TMPA): Quasi-global, multiyear, combined-sensor precipitation estimates at fine scales. *Journal of Hydrometeorology*, *8*(1), 38–55. https://doi.org/10.1175/JHM560.1

Jiang, S., Wei, L., Ren, L., Xu, C.-Y., Zhong, F., Wang, M., et al. (2021). Utility of integrated IMERG precipitation and GLEAM potential evapotranspiration products for drought monitoring over mainland China. *Atmospheric Research*, *247*, 105141. https://doi.org/10.1016/j.atmosres.2020.105141

Joyce, R. J., Janowiak, J. E., Arkin, P. A., & Xie, P. (2004). CMORPH: A method that produces global precipitation estimates from passive microwave and infrared data at high spatial and temporal resolution. *Journal of Hydrometeorology*, *5*(3), 487–503. https://doi.org/10.1175/1525-7541(2004)005<0487:camtpg>2.0.co;2

Kubota, T., Shige, S., Hashizume, H., Aonashi, K., Takahashi, N., Seto, S., & Okamoto, K. I. (2007). Global precipitation map using satellite-borne microwave radiometers by the GSMaP project: Production and validation. *IEEE Transactions on Geoscience and Remote Sensing*, *45*(7), 2259–2275. https://doi.org/10.1109/tgrs.2007.895337

Le, M.-H., Lakshmi, V., Bolten, J., & Du Bui, D. (2020). Adequacy of satellite-derived precipitation estimate for hydrological modeling in Vietnam Basins. *Journal of Hydrology*, *586*, 124820. https://doi.org/10.1016/j.jhydrol.2020.124820

Lenderink, G., de Vries, H., Fowler, H. J., Barbero, R., van Ulft, B., & van Meijgaard, E. (2021). Scaling and responses of extreme hourly precipitation in three climate experiments with a convection-permitting model. *Philosophical Transactions of the Royal Society A: Mathematical, Physical & Engineering Sciences*, *379*(2195), 20190544. https://doi.org/10.1098/rsta.2019.0544

Lenderink, G., & van Meijgaard, E. (2008). Increase in hourly precipitation extremes beyond expectations from temperature changes. *Nature Geoscience*, *1*(8), 511–514. https://doi.org/10.1038/ngeo262

Liu, J., Du, J., Yang, Y., & Wang, Y. (2020). Evaluating extreme precipitation estimations based on the GPM IMERG products over the Yangtze River Basin, China. *Geomatics, Natural Hazards and Risk*, *11*(1), 601–618. https://doi.org/10.1080/19475705.2020.1734103

Molina, M. O., Gutiérrez, C., & Sánchez, E. (2021). Comparison of ERA5 surface wind speed climatologies over Europe with observations from the HadISD dataset. *International Journal of Climatology*, *41*, 4864–4878. doi:10.1002/joc.7103

Panthou, G., Mailhot, A., Laurence, E., & Talbot, G. (2014). Relationship between surface temperature and extreme rainfalls: A multi-time-scale and event-based analysis. *Journal of Hydrometeorology*, *15*(5), 1999–2011. https://doi.org/10.1175/JHM-D-14-0020.1

Pumo, D., & Noto, L. V. (2021). Exploring the linkage between dew point temperature and precipitation extremes: A multi-time-scale analysis on a semi-arid Mediterranean region. *Atmospheric Research*, *254*, 105508. https://doi.org/10.1016/j.atmosres.2021.105508

Schroeer, K., & Kirchengast, G. (2018). Sensitivity of extreme precipitation to temperature: The variability of scaling factors from a regional to local perspective. *Climate Dynamics*, *50*(11–12), 3981–3994. https://doi.org/10.1007/s00382-017-3857-9

Skofronick-Jackson, G., Petersen, W. A., Berg, W., Kidd, C., Stocker, E. F., Kirschbaum, D. B., et al. (2017). The Global Precipitation Measurement (GPM) mission for science and society. *Bulletin of the American Meteorological Society*, *98*(8), 1679–1695. https://doi.org/10.1175/bams-d-15-00306.1

Smith, A., Lott, N., & Vose, R. (2011). The integrated surface database: Recent developments and partnerships. *Bulletin of the American Meteorological Society*, *92*(6), 704–708. https://doi.org/10.1175/2011bams3015.1

Sorooshian, S., Hsu, K.-L., Gao, X., Gupta, H. V., Imam, B., & Braithwaite, D. (2000). Evaluation of PERSIANN system satellite-based estimates of tropical rainfall. *Bulletin of the American Meteorological Society*, *81*(9), 2035–2046. https://doi.org/10.1175/1520-0477(2000)081<2035:eopsse>2.3.co;2

Tan, J., Huffman, G. J., Bolvin, D. T., & Nelkin, E. J. (2019). IMERG V06: Changes to the morphing algorithm. *Journal of Atmospheric and Oceanic Technology*, *36*(12), 2471–2482. https://doi.org/10.1175/jtech-d-19-0114.1

Tian, Y., Peters-Lidard, C. D., Eylander, J. B., Joyce, R. J., Huffman, G. J., Adler, R. F., et al. (2009). Component analysis of errors in satellite-based precipitation estimates. *Journal of Geophysical Research*, *114*, D24101. https://doi.org/10.1029/2009JD011949

Trenberth, K. E., Dai, A., Rasmussen, R. M., & Parsons, D. B. (2003). The changing character of precipitation. *Bulletin of the American Meteorological Society*, *84*(9), 1205–1218. https://doi.org/10.1175/BAMS-84-9-1205

Vergara-Temprado, J., Ban, N., & Schär, C. (2021). Extreme sub-hourly precipitation intensities scale close to the Clausius-Clapeyron rate over Europe. *Geophysical Research Letters*, *48*(3), e2020GL089506.

Visser, J. B., Wasko, C., Sharma, A., & Nathan, R. (2020). Resolving inconsistencies in extreme precipitation-temperature sensitivities. *Geophysical Research Letters*, *47*(18), e2020GL089723. https://doi.org/10.1029/2020GL089723

Westra, S., Fowler, H. J., Evans, J. P., Alexander, L. V., Berg, P., Johnson, F., et al. (2014). Future changes to the intensity and frequency of short-duration extreme rainfall. *Reviews of Geophysics*, *52*(3), 522–555. https://doi.org/10.1002/2014RG000464

Zhang, W., Villarini, G., & Wehner, M. (2019). Contrasting the responses of extreme precipitation to changes in surface air and dew point temperatures. *Climatic Change*, *154*(1–2), 257–271. https://doi.org/10.1007/s10584-019-02415-8

Zhang, X., Zwiers, F. W., Li, G., Wan, H., & Cannon, A. J. (2017). Complexity in estimating past and future extreme short-duration rainfall. *Nature Geoscience*, *10*(4), 255–259. https://doi.org/10.1038/ngeo2911

Zubieta, R., Getirana, A., Espinoza, J. C., Lavado-Casimiro, W., & Aragon, L. (2017). Hydrological modeling of the Peruvian–Ecuadorian Amazon Basin using GPM-IMERG satellite-based precipitation dataset. *Hydrology and Earth System Sciences*, *21*(7), 3543–3555. https://doi.org/10.5194/hess-21-3543-2017